Cement and Concrete Research 42 (2012) 27–38

Contents lists available at ScienceDirect

Cement and Concrete Research

journal homepage: http://ees.elsevier.com/CEMCON/default.asp

The effect of gyrolite additive on the hydration properties of Portland cement

A. Eisinas *, K. Baltakys, R. Siauciunas

Department of Silicate Technology, Kaunas University of Technology, Radvilenu 19, LT — 50270 Kaunas, Lithuania

ARTICLE INFO

Article history:
Received 30 June 2010
Accepted 18 July 2011

Keywords:
Calorimetry (A)
Calcium–silicate–hydrate (C–S–H) (B)
Hydration products (B)
Ordinary Portland cement (D)
Gyrolite

ABSTRACT

The influence of gyrolite additive on the hydration properties of ordinary Portland cement was examined. It was found that the additive of synthetic gyrolite accelerates the early stage of hydration of OPC. This compound binds alkaline ions and serves as a nucleation site for the formation of hydration products (stage I). Later on, the crystal lattice of gyrolite becomes unstable and turns into C–S–H, with higher basicity (C/S ~ 0.8). This recrystallization process is associated with the consumption of energy (the heat of reaction) and with a decrease in the rate of heat evolution of the second exothermic reaction (stage II). The experimental data and theoretical hypothesis were also confirmed by thermodynamic and the apparent kinetic parameters of the reaction rate of C_3S hydration calculations. The changes occur in the early stage of hydration of OPC samples and do not have a significant effect on the properties of cement stone.

1. Introduction

The early hydration kinetics of cement are of fundamental importance to understanding the behavior of cement-based materials, as they influence nano/microstructural evolution, setting time, dimensional stability, strength development, and durability. Despite the practical importance of the kinetics of cement hydration, early-age reactions of cement-based materials remain imperfectly understood [1–5]. Several mathematical models have been applied, however, to characterize the hydration kinetics of the principal component of Portland cement, C_3S [6–8]. The mechanism of hydration of individual cement components and that of cement itself has been a subject of much discussion and disagreement [9–21]. It is known that as soon as the C_3S comes into contact with water a significant amount of heat is generated because of the dissolution of species such as Ca^{2+} and OH^- ions in the aqueous phase. This stage is called the preinduction period. During the next few hours (the dormant, or induction, period), the rate of hydration is negligible. This period is followed by acceleration in the hydration process. The heat of hydration diminishes after about 10 h, during the deceleration stage.

Previous studies [17,22] have shown that the additive of amorphous silica and natural pozzolana accelerates the early stage of hydration of Portland cement and its individual compounds. The authors propose that the increased rate of hydration may be due to enhanced precipitation of hydration products on the surface of pozzolan, which possibly serves as a nucleation site during the first few hours, when it exists as chemically inert filler. It has been suggested that the surface of pozzolans can adsorb many Ca^{2+} ions and that lowering the concentration of calcium ions accelerates the rate of dissolution of C_3S [17,22].

There are several hypotheses for the mechanisms responsible for these stages [19–21,23].

Morin et al. [21] determined that the additive of ion-exchange resins in a paste of C_3S has a definite accelerating effect on early-age hydration. This acceleration is related to the abundant formation of C–S–H nuclei during the very first moments of the hydration process. In the longer term and depending on the amount of resin added to the C_3S, contradictory results may be obtained: that is, either the hydration process will slow down or, on the contrary, the degree of hydration of the C_3S will increase, compared with a reference sample without a resin additive.

Thomas et al. [19] proposed that silica-containing materials first react with calcium ions released by the dissolving cement or C_3S to form C–S–H, which then in turn seeds the hydration process. This explains why the effectiveness of these additives in stimulating the early hydration rate depends strongly on their solubility.

Hydration products of Portland cement are primary calcium silicate hydrate gels (C–S–H), which are a mixture of poorly crystallized particles. Thus, the properties of these gels are important for the mechanical and chemical properties of cement based materials. C–S–H gels are commonly formed via the hydration of C_3S and β-C_2S, which are the principal constituents of Portland cement clinker. In hardened cement pastes, C–S–H gels are nanoheterogeneous, showing variable composition on a micrometric scale [24].

The calcium silicate hydrates are an important group of silicate minerals with compositions varying over a large CaO/SiO_2 (C/S) range (0.44–3.0) and crystallographic structures ranging from amorphous to well-crystalline [24–28]. Among the different silicate minerals, calcium silicate hydrates are the prime candidates for heavy metal binding because of their abundance and appropriate structure [29–31].

* Corresponding author. Tel.: +370 7 300150; fax: +370 7 300152.
E-mail address: anatolijus.eisinas@ktu.lt (A. Eisinas).

0008-8846/$ – see front matter © 2011 Elsevier Ltd. All rights reserved.
doi:10.1016/j.cemconres.2011.07.003

Table 1
Chemical and mineralogical composition of clinker.

Oxides	SiO_2	Al_2O_3	Fe_2O_3	CaO	MgO	Na_2O	K_2O	SO_3^{2-}	Ignition of losses	Insoluble particles
Amount, %	19.72	5.41	4.21	62.76	3.41	0.16	1.08	2.08	0.93	0.24
Minerals	$3CaO \cdot SiO_2$		$2CaO \cdot SiO_2$		$3CaO \cdot Al_2O_3$			$4CaO \cdot Al_2O_3 \cdot Fe_2O_3$		
Amount, %	63.19		8.89		7.21			12.81		

Presumably, that gyrolite ($Ca_{16}Si_{24}O_{60}(OH)_8 \cdot 14 + xH_2O$) will have a better sorption capacity than other calcium silicate hydrates because the interlayer sheets in the structure, with a thickness of about 2.2 nm (one of the largest in all the calcium silicate hydrates group) are available for the intercalation of a new guest by controlling the charge of the host [32]. Gyrolite rarely occurs as a natural mineral in association with zeolites and often forms nodular aggregates. These aggregates can appear glassy, dull or even fibrous. One of the reasons that the properties of gyrolite have not been analyzed in detail is that the synthesis of this compound is complex, and it is still rarely applied in practice [32–37]. Some published works indicate that it is suitable for cleaning water from heavy metal ions, and its cation exchange capacity is better that of natural zeolites [38–41]. Therefore, gyrolite with substituted ions can be utilized in mixtures with Portland cement, but the influence of this compound on the properties of cement paste is unknown.

The main objective of the present work was to examine the influence of synthetic gyrolite additive on the hydration of Portland cement.

2. Materials and methods

2.1. Materials

In this study the following reagents for gyrolite synthesis were used as starting materials: fine-grained $SiO_2 \cdot nH_2O$ ("Reaktiv", Russia, ignition losses 21.28%, specific surface area $S_a = 1155$ m²/kg) and calcium oxide (CaO was burned at 950 °C for 0.5 h; $S_a = 548$ m²/kg; purity, 96%).

Samples of ordinary Portland cement were prepared in a laboratory grinding mill by grinding cement clinker (JSC "Akmenes cementas", Lithuania) with a 4.5% additive of gypsum ("Sigma-Aldrich", Germany) up to $S_a = 450$ m²/kg. The chemical analysis and phase composition of clinker are shown in Table 1.

2.2. Manufacture of synthetic gyrolite

Pure gyrolite was synthesized in the hydrothermal conditions after 48 h at 200 °C temperature from a stoichiometric composition (C/S = 0.66) of calcium oxide and SiO_2nH_2O mixture. Dry primary mixture was mixed with water in the vessels of stainless steel (water/solid ratio of the suspension W/S = 10.0). These synthesis conditions were chosen according to previously published data [36]. The product was filtered off, dried at 50 ± 5 °C, and put through a sieve with an 80-μm mesh.

2.3. Isothermal calorimetry

An eight channel TAM Air III isothermal calorimeter was used to investigate the heat evolution rate of OPC and OPC blended with 2.5%, 5% or 7.5% by weight of gyrolite. Glass ampoules (20 ml) each containing 3 g dry cementitious material were placed in the calorimeter and the injection units for each ampoule filled with amounts of water equivalent to a W/(OPC + additive) ratio of 0.5. After a steady temperature of 25 °C had been reached, the water was injected into the ampoules and mixed inside the calorimeter with the

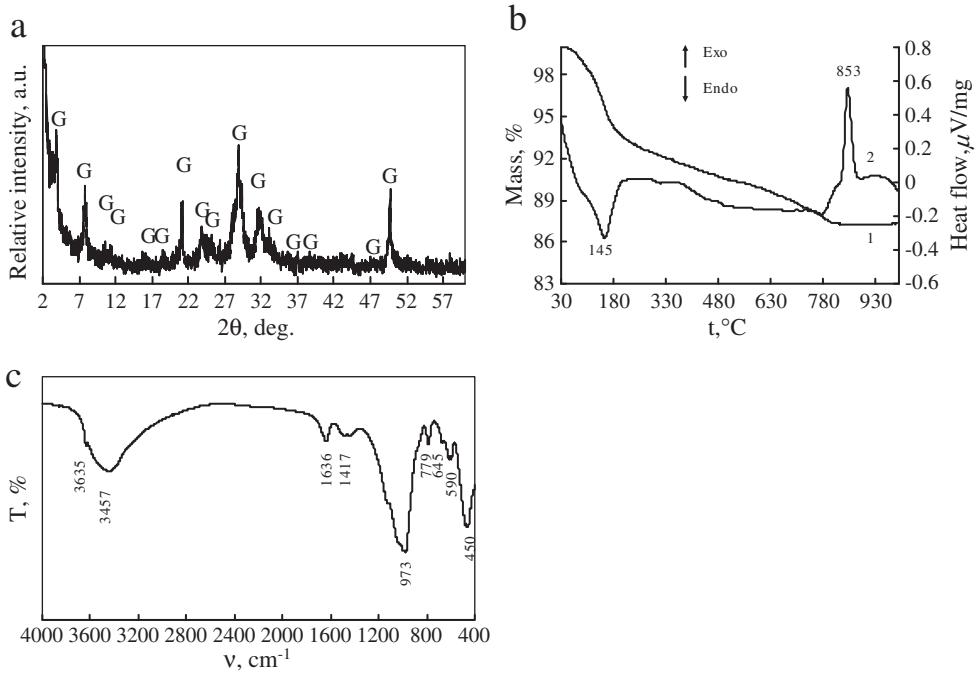

Fig. 1. X-ray diffraction pattern (a), STA curves (b, curve 1 — TG; curve 2 — DSC) and FT-IR spectrum (c) of pure gyrolite. The duration of hydrothermal synthesis at 200 °C is 48 h. Indexes: G — gyrolite.

Table 2
Calculated parameters of gyrolite specific surface area (S_{BET}).

Sample mass m, g	BET equation constants		Capacity of monolayer $X_m = \frac{1}{S+I}, g$	Specific surface area S_{BET}, m^2/g	Constant $C_{BET} = \frac{1}{I X_m}$	Reliability coefficient R^2
	Slope $S = tg\alpha$	Intercept I				
0.1127	437.83	0.9485	0.0023	71.02	462.603	0.9991

dry material for 20 s (frequency 2–3 s^{-1}). The heat evolution rate was then measured over a period of 72 h. Repetition of the measurements showed deviations in total heat below 3% for samples of similar type. Apart from the first minutes of water additive and mixing, the heat evolution rates were essentially identical.

2.4. Compressive strength of OPC samples

Samples for compressive strength analysis (prisms 4×4×16 cm) were formed following the standard EN 196-1 (the ratio of cement and sand was 1:3 by weight). Gyrolite was added as a partial replacement of the OPC at levels of 0%, 2.5%, 5% and 7.5% by weight of the total cementitious material. Therefore the water and cement ratio (W/C) of all OPC samples was equal to 0.5. During the first day, the samples are kept in molds at 20±1 °C and 100% air humidity. After 24 h of formation, the samples were transferred into distilled water and stored there for 6, 27 and 83 days at 20±1 °C. Hydration of samples was stopped by using acetone. After hardening the samples were crushed to powder, dried at the temperature of 50±5 °C and put through a sieve with an 80-μm mesh.

2.5. Analytical techniques

The surface area of synthetic gyrolite was performed by a BET surface area analyzer "KELVIN 1042 Sorptometer" (Costech Instruments). The specific surface area of gyrolite was calculated by the BET equation using the data of the lower part of N_2 adsorption isotherm ($0.05 < p/p0 < 0.35$):

$$\frac{1}{X\left(\frac{p_0}{p}-1\right)} = \frac{C-1}{X_m \cdot C}\cdot\frac{p}{p_0} + \frac{1}{X_m \cdot C},$$

where X is the mass of adsorbate, adsorbed on the sample at relative pressure p/p_0, p the partial pressure of adsorbate, p_0 the saturated vapor pressure of adsorbate, X_m the mass of adsorbate adsorbed at a coverage of one monolayer, C is a constant which is a function of the heat of the adsorbate condensation and heat of adsorption (C_{BET} is a constant).

Compressive strength of the samples was performed with "ELE International 250 kN Automatic Cement Compression Machine, EL39-1501/01 Autotest250" press. The data of compressive strength test were calculated as the arithmetic mean of the six individual results, each expressed at least to the nearest 0.1 MPa, obtained from the six determinations made on a set of three prisms.

The X-ray powder diffraction (XRD) data were collected with a DRON-6 X-ray diffractometer with Bragg–Brentano geometry using Cu K_α radiation and graphite monochromator, operating with the voltage of 30 kV and emission current of 20 mA. The step-scan covered the angular range of 2–60° (2θ) in steps of $2\theta = 0.02°$. The quantitative analysis (QXRD) of the phases in the samples was carried out with the Rietveld method (software Autoquan) by using XRD data.

The specific surface area of the raw materials was determined by the Blaine's method with air permeability apparatus (Model 7201, Toni Technik Baustoffprufsysteme GmbH).

Simultaneous thermal analysis (STA: differential scanning calorimetry — DSC and thermogravimetry — TG) was also employed for measuring the thermal stability and phase transformation of samples at a heating rate of 15 °C/min, the temperature ranged from 30 °C up to 1000 °C under air atmosphere. The test was carried out on a Netzsch instrument STA 409 PC Luxx. The ceramic sample handlers and crucibles of Pt-Rh were used.

FT-IR spectra have been carried out with the help of a Perkin Elmer FT-IR Spectrum X system. Specimen was prepared by mixing 1 mg of the sample with 200 mg of KBr. The spectral analysis was performed in the range of 4000–400 cm^{-1} with spectral resolution of 1 cm^{-1}.

3. Results and discussion

3.1. Characterization of synthetic gyrolite

The results of XRD studies confirmed that in the $CaO–SiO_2 \cdot nH_2O–H_2O$ system within 48 h at 200 °C, pure gyrolite was synthesized (Fig. 1, a).

On the DSC curve at 145 °C the broad endothermic peak is related to the loss of physisorbed and interlayer water from the crystal structure of gyrolite. The second exothermic peak (853 °C) is associated with recrystallization of this compound into wollastonite (Fig. 1, b).

All of these data were confirmed by method of FT-IR spectroscopy, which can be used to distinguish gyrolite from other calcium silicate hydrates. A sharp peak near 3635 cm^{-1}, which is visible only in the gyrolite spectrum, proves that clearly distinguished OH positions exist in the structure of gyrolite, which are connected only with Ca atoms and are not influenced by hydrogen bridge links. A wide band near 3457 cm^{-1}

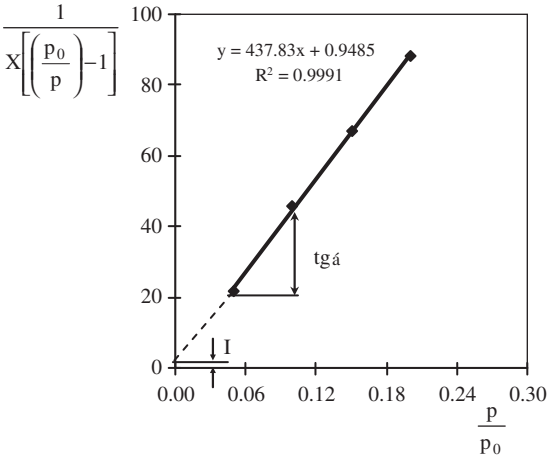

Fig. 2. The isotherm of N_2 adsorption by gyrolite at 77 K in BET plot.

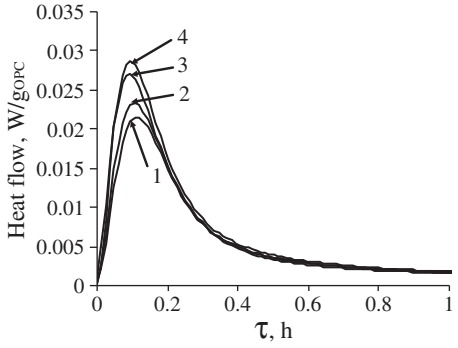

Fig. 3. Heat evolution rate of OPC samples during the early stage of hydration. Amount of additive, wt.%: 1 — 0; 2 — 2.5; 3 — 5; 4 — 7.5.

means the opposite that molecular water forms hydrogen bridge links in the interlayers. The bands in the range of 1636 cm^{-1} frequency are assigned to $\delta(H_2O)$ vibrations and confirm this presumption. Also, it was determined a doublet near ~590 and ~612 cm^{-1} due to Si–O–Si bending vibrations, the band at ~973 cm^{-1} due to the Si–O stretching mode of nonbridging oxygens, and the band at ~645 cm^{-1} due to the Si–O–Si bonds (Fig. 1, c).

The calculated parameters of the specific surface area (S_{BET}) of synthetic gyrolite are shown in Table 2. It was determined that a stable monolayer of absorbed N_2 was formed on the surface of gyrolite (Fig. 2).

The BET equation gives a linear plot in the range of relative pressures $0.05 \le p/p_0 \le 0.30$ (Fig. 2). Straight line was obtained for the gyrolite sample in BET coordination $\frac{1}{X\left[\left(\frac{p_0}{p}\right)-1\right]} - \frac{p}{p_0}$, and the straight-line correlation coefficient R^2 was equal to 0.9991 (Fig. 2).

It was found that gyrolite is a mesoporous material. Its specific surface area is found by $S_{BET} = 71.02$ m^2/g, and the radius of dominant plate pores is $r_p = 8$–9 nm.

3.2. Heat flow of cement paste. Adsorption properties and stability of gyrolite

The rate of heat evolution was calculated on the basis of a unit weight of ordinary Portland cement (OPC): thus, the rates can be compared with each other, and the contribution from the amount of gyrolite can be separated. The rate of heat evolution (W/g_{OPC}) and the cumulative heat of hydration (J/g_{OPC}) data of the binary blended pastes are presented in Figs. 3, 5, 6 and 7. The heat of hydration curves for pure OPC and OPC with additives show the typical five stages of the hydration reaction (the initial reaction, the induction period, the acceleratory period, the deceleratory period, and the period of slow continued reaction) as described in the literature. In the initial reaction, there is a rapid evolution of the heat culminating in a peak within the first 1–2 min. This was ascribed to the effects of the heat of wetting of the cement and hydration of free lime. In the first few minutes of hydration, there was a rapid release of Ca^{2+}, OH^-, $H_2SiO_4^{4-}$, SO_4^{2-}, and alkali ions from the cement compounds. It should be emphasized that hydration at this stage is accelerated by gyrolite because the first peak of all samples with this additive produces an increase of the maximum heat evolution rate relative to OPC, and this effect grows as the gyrolite level increases (Fig. 3).

Presumably, the additive of gyrolite accelerates the early stage of hydration of OPC and its individual compounds because of the adsorption reaction with both alkaline and calcium ions. For this reason, lowering the concentration of Ca^{2+} ions in the solution accelerates the rate of dissolution of C_3S. This aspect is in good agreement with the dissolution theory proposed by Juilland et al. [44] since the consumption of Ca^{2+} will keep a low undersaturation and therefore enable a higher rate of dissolution.

To show the adsorption properties of gyrolite, a mixture of gyrolite and portlandite (CH) with a molar ratio of C/S of 1.75, which corresponds to the main hydration product (calcium silicate hydrate gel), was prepared. Adsorption experiments were carried out at 25 °C in a Grant SUB14 thermostatic absorber by stirring 0.5 g of mixture in a aqueous solution (W/S — 10.0) for 1, 2, 3 or 7 min. Also, it was calculated that the initial mixture contained a 25.62% excess of calcium ions according to $Ca(OH)_2$ solubility (1.13 g CaO/1000 g H_2O). It is known that CH can exist in both crystalline and amorphous form during hydration of cement minerals. Various authors have shown thermal analysis techniques to be very reliable for estimating the CH content of set Portland cement [42,43]. In the present study, STA has been used to estimate the CH content at different times of adsorption.

Fig. 4 shows the adsorption capacity of gyrolite for CH after different times of the adsorption process. There is a clear trend toward an increment in the quantity of calcium ions in the gyrolite structure with prolonged adsorption time.

It has been noted that the intrusion of calcium ions proceeds intensively in the first minute of the adsorption process. The amount of adsorbed Ca^{2+} ions in the crystals lattice of gyrolite after 1 min is

Table 3
The main characteristics of thermal effects typical of gyrolite and portlandite.

	Onset, °C	Peak, °C	Area, J/g	Weight loss (%)
Duration of adsorption with endothermic peak at 140 °C, min				
0	109	136	30.9	3.61
1	111	135	30.3	3.55
2	110	136	29.8	3.79
3	112	137	30.1	3.50
5	109	134	30.6	3.61
7	110	136	30.8	3.53
Duration of adsorption with endothermic peak at 450 °C, min				
0	382	421	2328.2	24.34
1	380	419	327.5	3.41
2	379	420	285.9	3.00
3	380	417	264.6	2.77
5	380	419	251.2	2.63
7	381	420	238.7	2.50

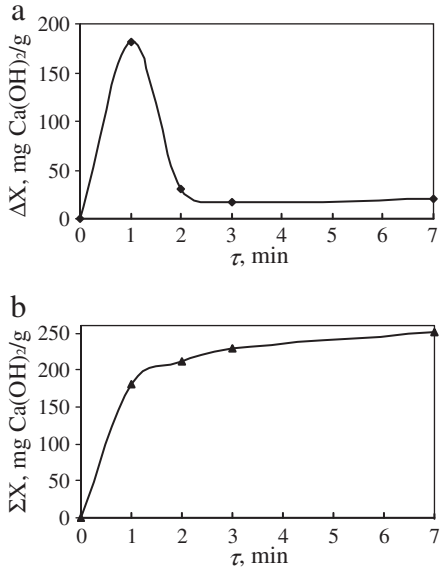

Fig. 4. Differential (a) and integral (b) kinetic curves of $Ca(OH)_2$ adsorption by gyrolite at 25 °C.

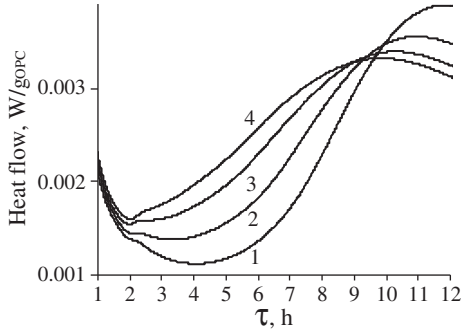

Fig. 5. Heat evolution rate of OPC samples for the following amounts of additive, wt.%: 1 — 0; 2 — 2.5; 3 — 5; 4 — 7.5.

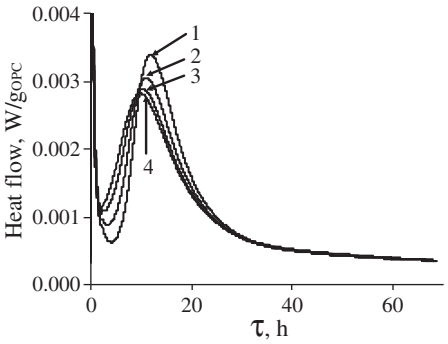

Fig. 6. The influence of the amount of gyrolite on the rate of heat evolution of OPC samples for the following amounts of additive, wt.%: 1 — 0; 2 — 2.5; 3 — 5; 4 — 7.5.

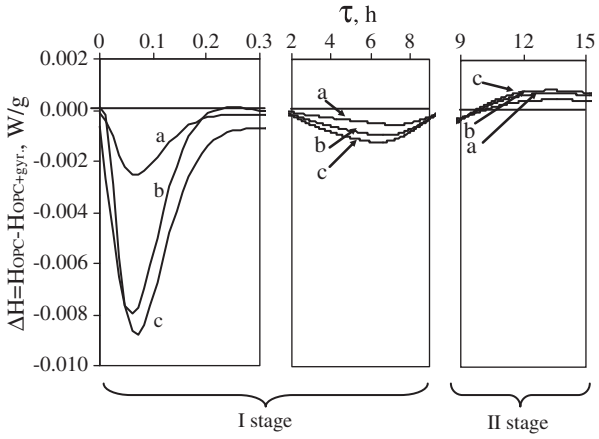

Fig. 7. The differences between heat evolution of samples of pure OPC and OPC with the additive of gyrolite for the following amounts of additive, wt.%: a — 2.5; b — 5; c — 7.5.

182 mg $Ca(OH)_2$/g (Fig. 4). With a longer adsorption process, the reaction rate greatly decreases, and after 7 min, the amount of Ca^{2+} ions incorporated into the crystal structure of gyrolite grew only to 248 mg $Ca(OH)_2$/g (Fig. 4).

During adsorption, interlayers of gyrolite structure are evidently sufficiently porous that calcium ions can migrate through them until equilibrium of the C/S ratio is reached. It should be noted that adsorption proceeds very quickly, and the limiting factor of this process is solubility of initial compounds in the solution. Incidentally, the initial reactions of OPC hydration are also rapid.

It was determined that the adsorption reactions are not a reversible process and are specific to the chemisorption process. To confirm this fact, after the adsorption process (25 °C, 7 min), the Ca-substituted gyrolite was dried and immersed in distilled water. It has been observed that Ca^{2+} ions are not released from the crystal lattice of gyrolite into solution during desorption.

In order to identify the stability of gyrolite, the products of adsorption were characterized by the STA method. It was determined that during the adsorption process, the identified area of endothermic effect at 140 °C does not change and it is equal to ~30.4 J/g (according to the linear method). It is clearly visible that the area of endothermic effect typical of CH decomposition at 420 °C decreased from 2328.2 J/g to ~238.7 J/g (Table 3).

The main characteristics of the thermal effects and mass losses mentioned here are presented in Table 3.

It should be noted that at the beginning of the adsorption process, the crystal structure of synthetic pure gyrolite is stable in CH solution when the molar ratio of C/S is equal to 1.75. The influence of the gyrolite and OPC replacement levels on the very early (induction period) rates of hydration is presented in Fig. 5. The induction period associated with pure OPC paste hydration is about 2.5 h, compared with only 20–30 min for a sample with 7.5% gyrolite.

Thus, in the samples with gyrolite, the induction period is effectively eliminated because this compound serves as a nucleation site (for growing C–S–H and CH on the surface of the particles of gyrolite) for the formation of hydration products.

The present results are only in partial agreement with the data of Thomas et al. [19], which discussed a general theory by which fine additives such as silica fumes, colloidal silica, and especially pure C–S–H stimulate the nucleation and growth kinetics by seeding the hydration reaction. In general, such additives increase the size (i.e. height and area) of the main hydration peak. Meanwhile, in our case, it was determined that gyrolite decreases the heat evolution rate of the second exothermic reaction, and as the amount of this additive increases in the samples, the accelerating effect begins earlier: from 2 h in samples with 7.5% additive to 4.5 h in pure OPC samples (Figs. 5 and 6).

Presumably, the decrease in the rate of heat evolution is associated with destruction of the crystal lattice of gyrolite (stage II) (Fig. 7). The experimental data and theoretical hypothesis were also confirmed by thermodynamic calculations. They were carried out using the method

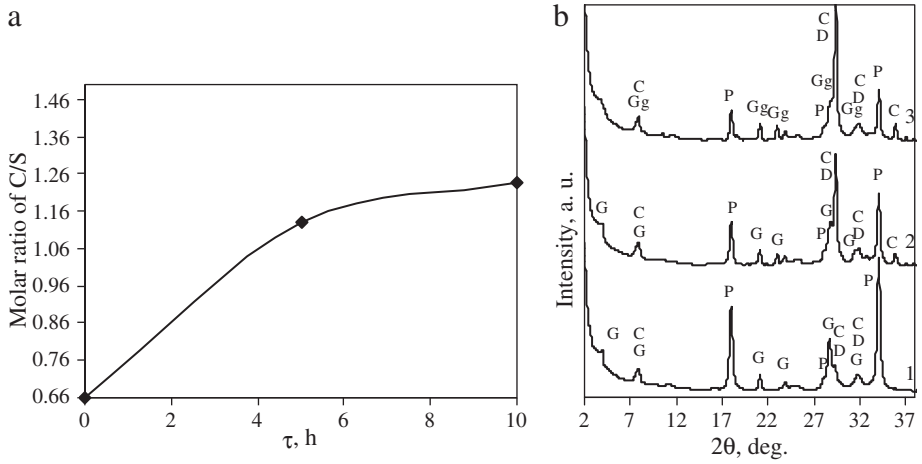

Fig. 8. Variation of C/S molar ratio (a) and X-ray diffraction pattern (b) of the gyrolite and CH mixture at an initial molar ratio of C/S = 1.75, W/S = 10.0, t = 25 °C, and the following durations of hydration, h: 1 — 0 (after mixing); 2 — 5; 3 — 10. Indexes: G — gyrolite; Gg — gyrolite gel; P — portlandite; C — calcium silicate hydrates (C/S ratio in this phase varies from 0.8 to about 1.3); D — calcium silicate hydrates (C/S: 1.3–2.0).

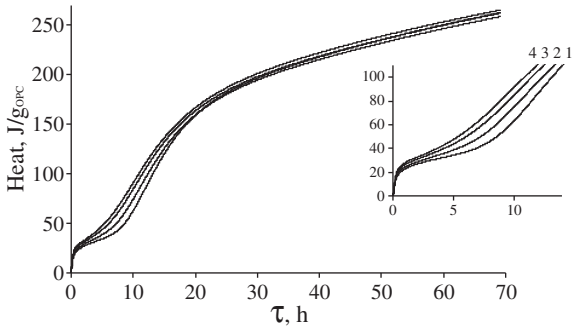

Fig. 9. The influence of gyrolite amount on the cumulative heat of OPC samples when the amount of additive was as follows, wt.%: 1 — 0; 2 — 2.5; 3 — 5; 4 — 7.5.

of V. I. Babushkin et al. [45]. From a thermodynamic point of view, the quantity of cumulative heat of OPC sample hydration is sufficient to destroy the crystal structure of gyrolite because the enthalpy of this compound is $\Delta H_f = -4914.42$ kJ/mol. These facts allow us to state that at the beginning of the experiments, the crystalline part of gyrolite remains stable, and only after 8–9 h of hydration does this compound recystallizes into C–S–H with higher basicity (C/S~0.8). This effect is clearly visible in Fig. 8, a, which shows a variation of the C/S molar ratio of the hydration products when the initial mixture consists of gyrolite and CH with C/S = 1.75. It was calculated that after 10 h of hydration, the C/S molar ration of products grows to C/S = 1.23 (Fig. 8, a). These data were confirmed by XRD results (Fig. 8, b). It should be noted that after 10 h of hydration, the main diffraction peak with *d*-spacing of 2.231, characteristic of gyrolite, was not identified. In the dominant products were semicrystalline calcium silicate hydrates with a C/S ratio of 0.8–2.0. Also, this phenomenon was confirmed by a decrease in the rate of heat evolution (stage II) (Fig. 7).

At later stages of hydration, gyrolite affects in the OPC hydration as the usual pozzolanic additives because the amount of cumulative heat grows with the increasing amount of gyrolite in the samples (Fig. 9).

3.3. Quantity of portlandite in the cement paste

In order to prove a positive influence of gyrolite on CH formation, the quantity of the latter compound was determined in the hydration products. For this reason, the heat evolution experiments were repeated at different time period under normal conditions. Hydration of samples was stopped by using acetone. Later on, the samples were crushed to powder, dried at the temperature of 50 ± 5 °C and put through a sieve with an 80-μm mesh.

Fig. 10 shows DSC, TG and DTG curves of samples of pure OPC and OPC with gyrolite additive after 2 h (beginning of the acceleration period in OPC samples with 7.5% gyrolite) and 5 h (beginning of the acceleration period in pure OPC samples) of hydration.

The data obtained show the significant differences between mass losses typical of $Ca(OH)_2$ in the temperature range of 400–475 °C after only 2 h of hydration of all samples: as the amount of gyrolite in the samples increased, the mass losses grew from 0.27% (1.11% of $Ca(OH)_2$) to 0.89% (3.66% of $Ca(OH)_2$), respectively (Fig. 13). These data are in good agreement with the DSC results (Table 4).

Although TG curves are similar in shape, significant differences can be observed in both DSC and DTG profiles of portlandite decomposition. The dehydration profile of portlandite from OPC with additive samples is broader than the corresponding profile from pure OPC and exhibits lower onset temperature (Fig. 10, curve 1, 420 °C and 430 °C, respectively). Portlandite peak decomposition temperatures shift to higher temperatures (from 447 °C to 451 °C) in samples with additive. Presumably, that this trend depends on morphology of portlandite crystals. The same effect was observed after 5 h of hydration (Table 4). In this case, the mass losses increased from 0.60% (2.47% of $Ca(OH)_2$ in pure OPC samples) to 1.4% (5.76% of $Ca(OH)_2$ in samples with 7.5% of additive). After 5 h, DSC and DTG profiles of portlandite from all samples follow a trend similar to that after 2 h of hydration. Also, with an increasing amount of gyrolite in samples, the decomposition peak of portlandite shifts to higher temperatures (DSC_{max} from 449 to 452 °C; DTG_{max} from 438 to 442 °C).

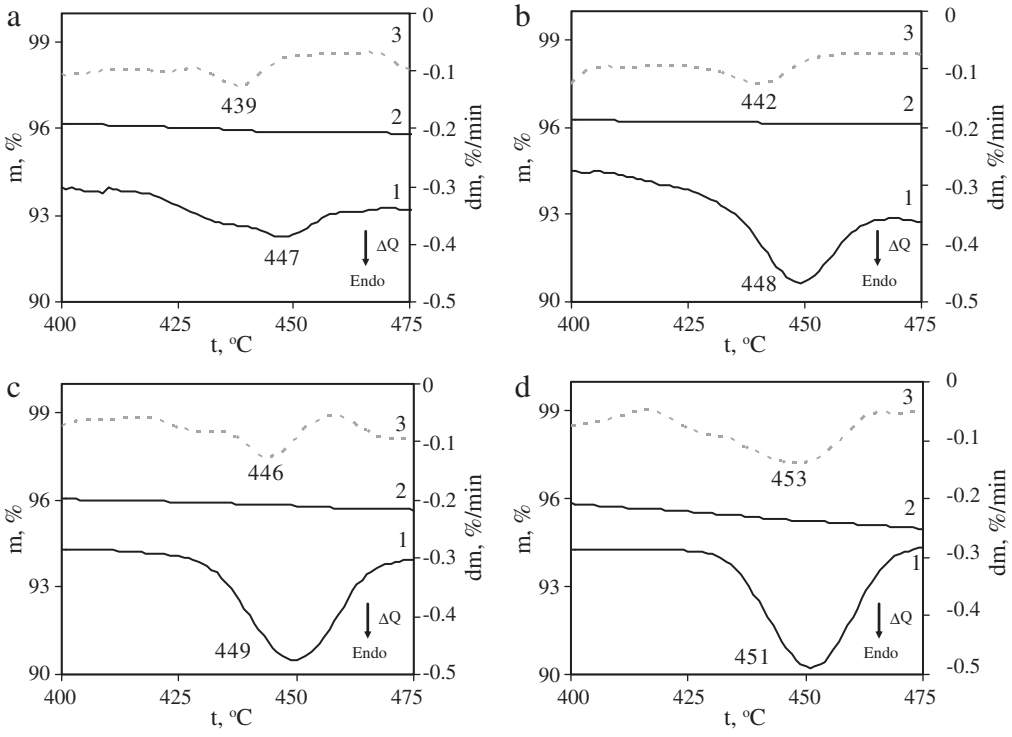

Fig. 10. DSC (curve 1), TG (curve 2) and DTG (curve 3) curves of samples of pure OPC and OPC with gyrolite additive after 2 h of hydration with the following amounts of additive, wt.%: a — 0; b — 2.5; c — 5; d — 7.5.

Table 4
Quantity of portlandite in the cement paste during hardening.

Duration of hydration, h	Amount of additive in samples of pure OPC, %	Data according to the TGA method		Data according to the DSC method	
		Mass losses at 400–475 °C, %	$W_{(Ca(OH)_2)}$,%	Peak area at 400–475 °C, J/g	$W_{(Ca(OH)_2)}$,%
2	0	0.27	1.11	118.61	1.24
	2.5	0.45	1.85	175.05	1.83
	5	0.57	2.34	219.05	2.29
	7.5	0.89	3.66	352.01	3.68
5	0	0.60	2.47	240.09	2.51
	2.5	0.82	3.37	323.31	3.38
	5	1.16	4.77	448.62	4.69
	7.5	1.40	5.76	551.93	5.77
9	0	1.24	5.09	481.14	5.03
	2.5	1.55	6.38	613.15	6.41
	5	1.57	6.44	615.06	6.43
	7.5	1.65	6.77	639.93	6.69
12	0	1.78	7.31	701.15	7.33
	2.5	1.81	7.44	704.98	7.37
	5	1.82	7.49	719.33	7.52
	7.5	1.88	7.73	743.24	7.77

Results of XRD confirm these results and show that increasing the quantity of portlandite in the samples increases the intensity of the peaks (Fig. 11).

3.4. Kinetics and modeling of the hydration process

The kinetics of cement hydration is concerned with the relationships between the degree of hydration α and the age τ and with the factors that influence them. It is known that α may relate either to an individual phase or to the cement as a whole. Because cement is a mixture of phases that react at different rates, there are problems in determining, and even in defining, α for the whole cement.

In this report, α was obtained by summing the amounts of C_3S that have reacted after heat evolution experiments at different time period under normal conditions. Firstly, the quantity of unreacted C_3S was determined by QXRD (Table 5). The quantity of C_3S was calculated from the intensity change of the basic reflection (*d*-spacing — 0.2604 nm). Each calculation was done five times, and it was determined that their data declined no more than ±5% from the mean. C_3S quantity in the mixtures of pure OPC and OPC with additives (before hydration) was equal to 100% (Fig. 12, Table 5).

Table 5
Unreacted C_3S quantity as a function of amount of gyrolite additive and time of hydration.

Hydration time (h)	C_3S residue quantity (parts of the unit) and amount of gyrolite additive (%)			
	0%	2.5%	5%	7.5%
2	0.92	0.70	0.68	0.64
5	0.88	0.68	0.65	0.63
9	0.63	0.63	0.60	0.60
12	0.56	0.55	0.54	0.53

It was determined that after 2 h of hydration, only 8% of C_3S reacts in pure OPC samples (Fig. 12). The further reduction of its quantity depends on duration of hydration (Table 5).

Meanwhile, in samples with 7.5% gyrolite additive, 0.36 of this compound was reacted after only 2 h (Fig. 12). It was noticed that gyrolite stimulates the earliest C_3S hydration in all samples. It was determined that after 12 h in all samples, there remained almost the same quantity of this compound (0.56–0.53, Table 5).

According to the kinetic equation of chemical process [46], the reaction rate $k_{app.}$ increases due to $f(c)^n$variation:

$$W = \frac{dx}{d\tau} = k(f(c)^n), \quad (1)$$

where k is the constant of reaction rate, $f(c)^n$ is the influence of reagents concentration on the reaction rate (W).

Linear form of Eq. (1) is:

$$ln\ W = ln\ k_{app.} + n_{app.} \cdot \ln(X_o - X_\tau), \quad (2)$$

where $W = dX/d\tau$ is reaction rate as reacted amount of C_3S, $k_{app.}$ is the apparent reaction rate constant, $n_{app.}$ is apparent order of reaction, X_o is initial amount of C_3S, and X_τ is residual amount of C_3S at reaction time τ.

On the basis of the data obtained (Table 5), apparent kinetic parameters of the total process of C_3S hydration were calculated (Fig. 13) according to the second equation.

It was established that the process rate as a function of $(X_o - X_\tau)$ in logarithmic plot gives a straight line (Fig. 14).

The slope and intercept of these plots determine the values of $n_{app.}$ and $\ln k_{app.}$, respectively. The values of reaction order and rate constant are given in Table 6.

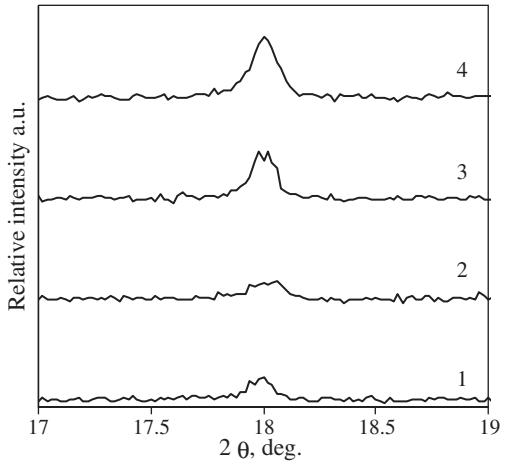

Fig. 11. The change of the main diffraction peaks of $Ca(OH)_2$ (*d*-spacing — 0.489 nm) after 5 h of hydration for the following amounts of additive, wt.%: 1 — 0; 2 — 2.5; 3 — 5; 4 — 7.5.

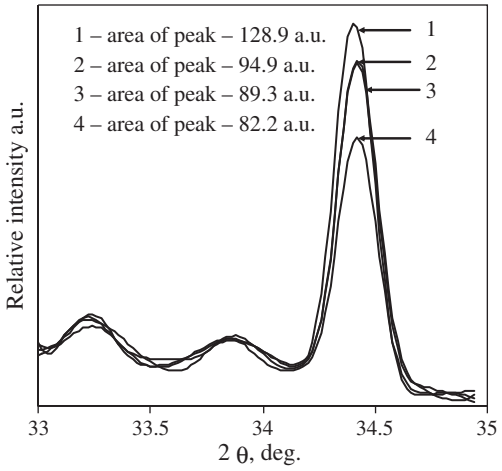

Fig. 12. The change of the main diffraction peak of C_3S (*d*-spacing — 0.260 nm) after 2 h of hydration with the following amounts of additive, wt.%: 1 — 0; 2 — 2.5; 3 — 5; 4 — 7.5.

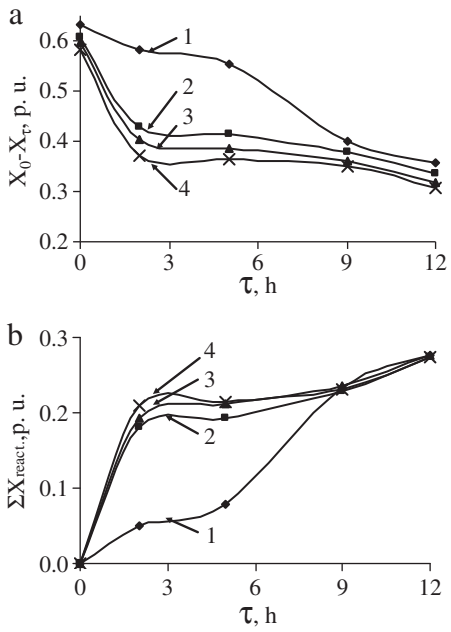

Fig. 13. Kinetic curves of residual amount of C_3S ($X_o - X_\tau$) (a) and amount of reacted C_3S (b) during OPC hydration with the following amounts of additive, wt.%: 1 — 0; 2 — 2.5; 3 — 5; 4 — 7.5.

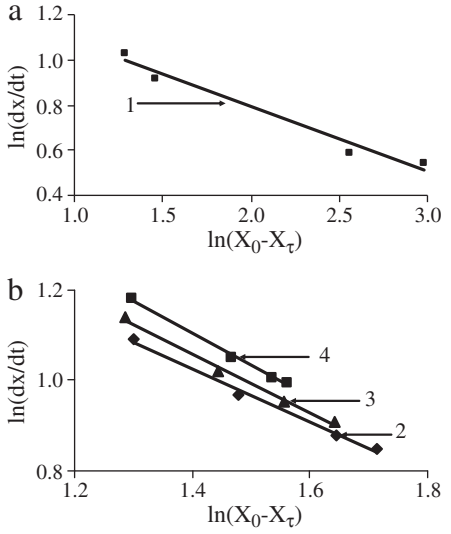

Fig. 14. Reaction rate of C_3S as a function of ($X_o - X_\tau$) in logarithmic plot during OPC hydration. a — pure OPC (1 curve); b — OPC with gyrolite additive, wt.%: 2 — 2.5, 3 — 5, 4 — 7.5.

The data obtained led us to conclude that additive of gyrolite changed the apparent kinetic parameters of the reaction rate of C_3S hydration. The following apparent kinetic parameters of mentioned process were estimated: when the amount of gyrolite was increased in the OPC samples, the reaction order $n_{app.}$ grew about 2.5 times (from 0.288 to 0.716), and the reaction rate $k_{app.}$ increased about 2 times (from 3.88 to 8.11), (Fig. 14, Table 6).

Table 6
Apparent kinetic parameters of reacted C_3S during OPC hydration.

Amount of additive, %	0	2.5	5	7.5
$k_{app.}$	3.88	6.28	7.07	8.11
$n_{app.}$	0.288	0.588	0.650	0.716
R^2	0.972	0.993	0.993	0.997

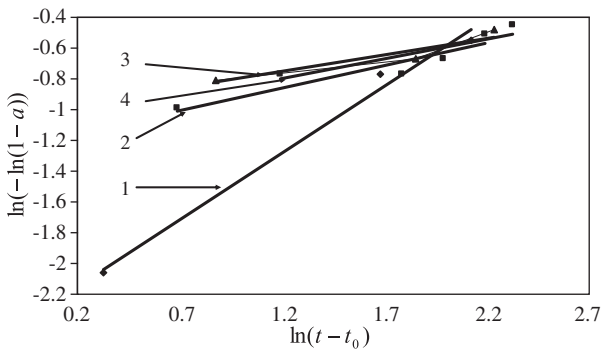

Fig. 15. Determination of n and k using the Avrami model in logarithmic scale during pure OPC hydration (1 curve) and OPC with gyrolite additive, wt.%: 2 — 2.5, 3 — 5, 4 — 7.5.

In order to describe the mechanism of OPC samples hydration, the calculated apparent kinetic parameters were fitted in the common hydration models. The most suitable model of OPC hydration is the one whose equation yields a straight line in linear form. It's known that hydration OPC process occurs by nucleation and growth, as well as by diffusion [2–8]. Therefore, the early-age hydration rate for C_3S was calculated according to two models: the Avrami (sometimes also denoted as the "JMAK" model) nucleation and growth model and the Jander diffusion model.

A general form of Avrami equation can be written as:

$$-\ ln(1-a)^{n_a} = k_a(t-t_0), \tag{3}$$

where a is the reacted fraction, k is the constant of reaction rate, t is time, t_0 is the induction time and n is a constant. Linear form of Avrami equation is:

$$ln(-\ ln(1-a)) = -\frac{ln\ k_a}{1} - \frac{1}{n_a}\cdot ln(t-t_0), \tag{4}$$

Fig. 15. shows a plot of the Avrami equation in logarithmic scale. From the slope of the resulting line the reaction order n_a was calculated (Table 7). Knowing n_a, a mean value for k_a can be obtained by calculating the reaction rate constant during OPC hydration with different amounts of gyrolite additive (Table 6).

Based on the Jander's model, the hydration reaction can be written as:

$$\left(1-(1-a)^{1/3}\right)^{n_j} = k_j t, \tag{5}$$

where, a is degree of hydration, k_j is the constant of reaction rate, t is hydration time, and n_j varies according to type of reaction governing the process. The value of n is calculated by plotting $\ln(1-(1-a)^{1/3})$ vs. ln(t) and determining the slope ($1/n_j$). When $n_j < 1$ the process occurs through nucleation, when $n_j = 1$ by phase boundary kinetics and when $n_j = 2$, by diffusion.

Fig. 16 shows the application of the Jander equation to the experimental data, while Table 8 summarizes the kinetic parameters.

It was determined that by using Avrami equation, the coefficient of determination R^2 (0.99) is acceptable only for pure OPC samples. Upon increasing the amount of gyrolite in the samples, the coefficient

Table 7
Apparent kinetic parameters of reacted C_3S during OPC hydration calculated by Avrami model.

Amount of additive, %	0	2.5	5	7.5
$k_{a.}$	0.069	0.016	0.009	0.013
$n_{a.}$	0.866	0.292	0.217	0.253
R^2	0.990	0.901	0.888	0.893

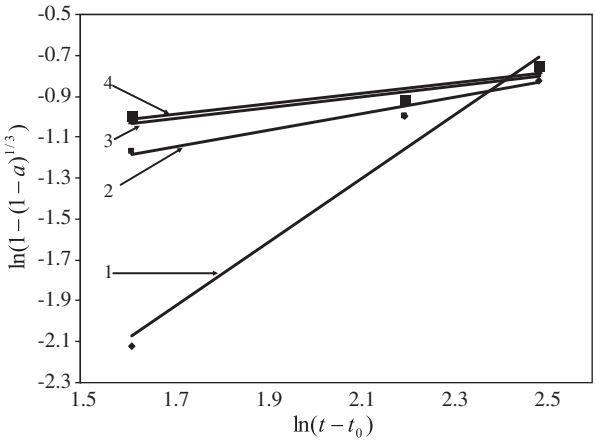

Fig. 16. Determination of n and k using the Jander model in logarithmic scale during pure OPC hydration (1 curve) and OPC with gyrolite additive, wt.%: 2 — 2.5, 3 — 5, 4 — 7.5.

determination R^2 appeared to be significantly lower (from 0.901 till 0.888). Meanwhile, it was estimated that by using Jander equation, the coefficients of determinations R^2 are acceptable not only for pure but also with additive OPC samples. Moreover, in pure OPC samples, the constant n_j is less than 1, indicating the reaction occurs by a nucleation kinetics. However, in OPC samples with gyrolite additive, the n_j values are >2, a value typical for diffusion controlled processes.

On the basis of the obtained results it can be assumed that gyrolite additive has effect on the OPC hydration mechanism.

3.5. Peculiarities of the process mechanism

As mentioned above, in the first few minutes of hydration (stage I), some of the alkaline and alkaline earth ions penetrate into the gyrolite structure, causing the dissolution of individual phases of cement to proceed faster. In order to prove penetration of mentioned ions, the adsorption properties of gyrolite were determined (Table 9). For this reason, the heat evolution experiments were repeated at different time period (1, 3, 5, 7 and 10 min) under normal conditions. A liquid phase during OPC hydration was collected by vacuum filtration. Due to adsorption properties of gyrolite, both Al^{3+}(<0.005 mg/dm^3) and Fe^{3+} ions (<0.045 mg/dm^3) were not identified in the liquid phase of

Table 8
Apparent kinetic parameters of reacted C_3S during OPC hydration calculated by Jander model.

Amount of additive, %	0	2.5	5	7.5
k_j	0.007	0.389	0.875	0.959
n_j	0.646	2.455	3.772	3.961
R^2	0.958	0.950	0.926	0.917

Table 9
Dependence of Al^{3+}, Ca^{2+} and Fe^{3+} ions concentrations on duration of hydration.

Duration of hydration, min.	Pure OPC samples			OPC with 7.5% gyrolite additive samples		
	Al^{3+} mg/dm^3	Ca^{2+} mg/dm^3	Fe^{3+} mg/dm^3	Al^{3+} mg/dm^3	Ca^{2+} mg/dm^3	Fe^{3+} mg/dm^3
1	<0.005	660.2	<0.045	<0.005	585.3	<0.045
3		580.9			574.6	
5		495.7			576.9	
7		485.1	0.134		586.1	
10		535.6	0.108		594.1	

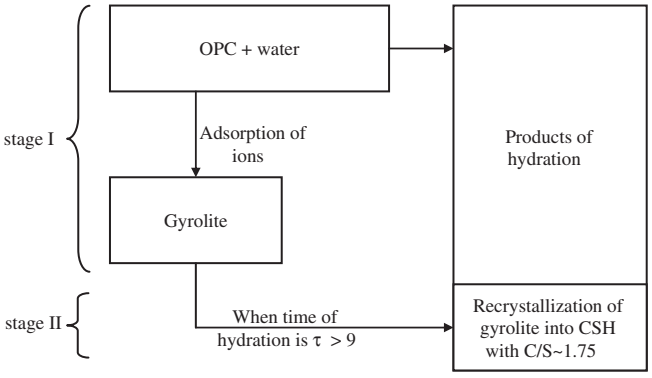

Fig. 17. Peculiarities of the hydration mechanism.

OPC samples with gyrolite additive. Also, a smaller amount of Ca^{2+} ions was observed at the beginning of hydration. It should be underlined that in pure OPC samples Fe^{3+} ions (0.134 mg/dm^3) were identified after 7 min of hydration (Table 9). Thus, the obtained results allow us to state that at the beginning of hydration alkaline ions penetrates into the gyrolite structure.

At later time, the added gyrolite acts as a nucleation site for hydration products. Incidentally, gyrolite is a metastable compound that recystallizes into C–S–H with higher basicity (C/S~0.8).

This process is schematically shown in Fig. 17, which shows a hypothesis of the suggested mechanism.

3.6. Effects of gyrolite on compressive strength of OPC

To evaluate the quality of OPC samples, the influence of synthetic gyrolite additive on the strength properties of OPC was determined. The results are shown in Fig. 18.

It was determined that gyrolite plays a dual role in the strength properties of cement paste: with a greater amount of additive, the intensive C_3S hydration reaction starts earlier, but on the other hand, it is not cementitious material; that is, this additive by itself has no binding properties. Thus, after 7 days of hydration, the maximum compressive strength (52 MPa) was shown by samples of OPC with 2.5% gyrolite additive, while the compressive strength (45 MPa) of samples containing 5% and 7.5% gyrolite remained only slightly higher than that of OPC samples (Fig. 18). After 28 and 84 days of hardening the samples containing any amount of gyrolite had a higher compressive strength than OPC samples.

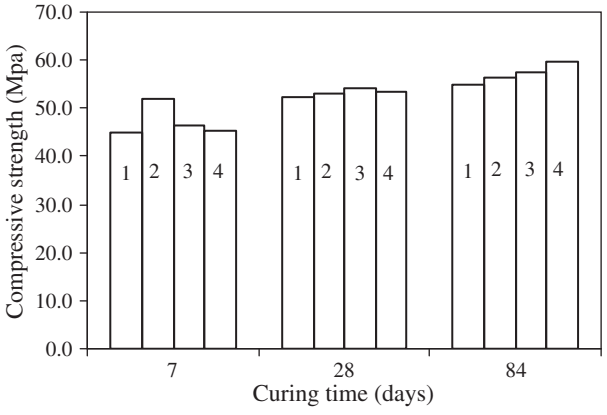

Fig. 18. Compressive strength of OPC samples vs. curing time with the following amounts of additive, wt.%: 1 — 0; 2 — 2.5; 3 — 5; 4 — 7.5.

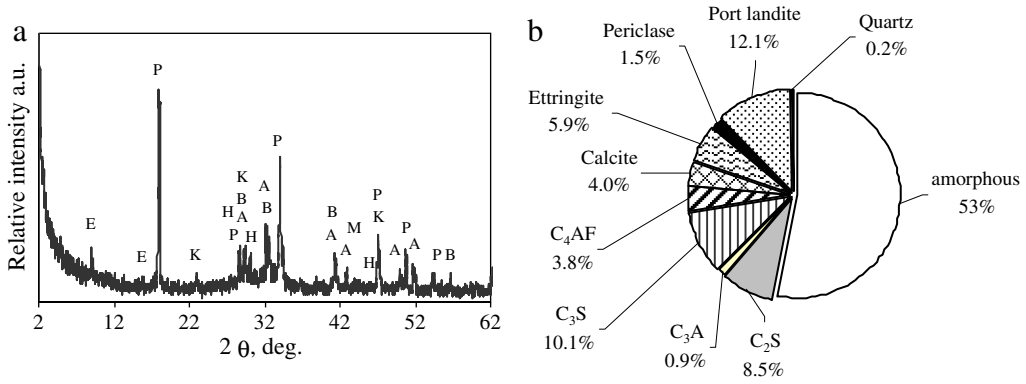

Fig. 19. X-ray diffraction pattern (a) and Rietveld quantitative analysis (b) of OPC sample cured for 28 days at 20 °C. Indexes: K — calcite; P — portlandite; A — alite; B — belite; E — ettringite; M — periclase; H — calcium silicate hydrates.

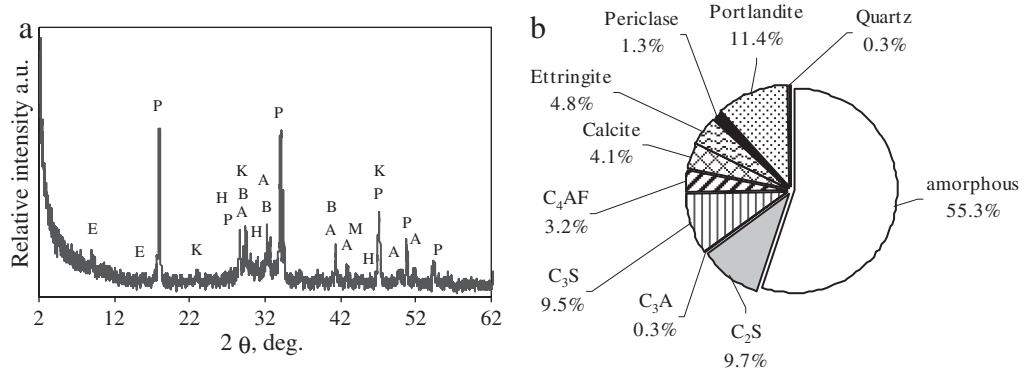

Fig. 20. X-ray diffraction pattern (a) and Rietveld quantitative analysis (b) of OPC with 5 wt.% gyrolite additive sample cured for 28 days at 20 °C. Indexes: K — calcite; P — portlandite; A — alite; B — belite; E — ettringite; M — periclase; H — calcium silicate hydrates.

3.7. Mineralogical analyses of OPC samples

To explain the strength properties of samples, XRD and STA analyses of the hydrated samples were carried out.

The XRD and Rietveld quantitative data are provided in Figs. 19 and 20. After 28 days of hydration in all samples the peaks of portlandite and calcium carbonate were determined. In addition, the diffraction peaks characteristic of calcium silicate hydrates, periclase and ettringite were identified. Unhydrated primary synthesis products, such as that of C_3S and C_2S were also seen in all samples.

The results of Rietveld quantitative analyses show very slight differences between samples of pure OPC and OPC with 5% of gyrolite after 28 days of hydration (Figs. 19, b and 20, b). It can be concluded that gyrolite has no significant influence on the mineralogical composition of OPC.

A simultaneous thermal analysis was performed for studies of cement hydration after 7 and 28 days of hydration. Three major peaks were observed in DSC curves consistently for both times (Fig. 21). The first endothermic peak at 50–150 °C is the result of dehydration reactions due to the loss of water from C–S–H and aluminates products. The second major peak, at 400–500 °C, corresponds to the dehydroxylation of $Ca(OH)_2$, another hydration product. The peak at

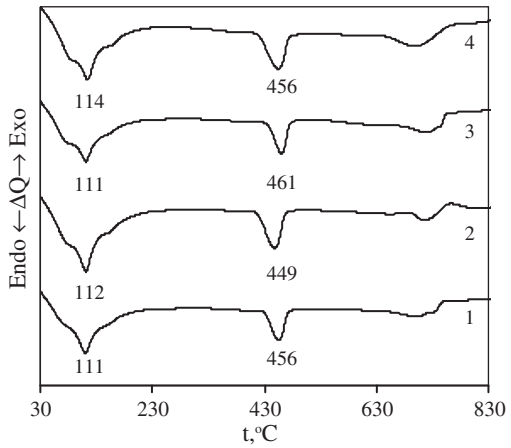

Fig. 21. DSC curves of OPC samples after 28 days of hydration with the following amounts of additive, wt.%: 1 — 0; 2 — 2.5; 3 — 5; 4 — 7.5.

Table 10
TG mass losses of samples of pure OPC and OPC with gyrolite additive after 7 and 28 days of hydration.

Hardening time, days	Amount of additive, wt.%	TG mass losses, %		
		50–150 °C	400–500 °C	650–800 °C
7	0	7.4	2.6	3.2
	2.5	8.2	3.4	4.8
	5	7.6	2.7	3.7
	7.5	7.7	2.7	3.7
28	0	12.4	2.9	4.3
	2.5	12.6	3.7	3.3
	5	14.8	3.7	4.9
	7.5	13.2	3.2	4.2

650–800 °C corresponds to the decarbonation of calcium carbonate. Mass losses of TG analyses are listed in Table 10.

One of the major differences between the hydration samples of pure OPC and OPC with gyrolite additive is the amount of calcium silicate hydrates and portlandite formed (Table 10). After 7 days of curing in water, the greatest amount of $Ca(OH)_2$ was observed in the samples with 2.5% of gyrolite additive.

It was determined that after 28 days of hydration, the largest mass losses (14.8%) during the dehydration of C–S–H were from the sample with 5% of gyrolite. Meanwhile, samples of pure OPC and OPC with 2.5% additive lost slightly less weight (12.6%). Thus, it can be stated that most of the calcium silicate hydrates had formed in OPC samples with 5% of gyrolite after 28 days of hydration. These data agree with results of strength properties of samples. Also, TG results show similar amounts of portlandite and calcite formed.

4. Conclusions

1. Synthetic pure gyrolite prepared under hydrothermal conditions (C/S = 0.66; 48 h; 200 °C; S_{BET} = 71.01 m^2/g; r_p = 8–9 nm) acts as chemisorbent in mixtures with portlandite. The adsorption proceeds very fast, and the limiting factor of this process is solubility of the initial compounds in the solution. It was determined that the amount of adsorbed Ca^{2+} ions in the crystal lattice of gyrolite after 1 min is equal to 182 mg of $Ca(OH)_2$/g. With a longer duration of the adsorption process, the reaction rate greatly decreases, and after 7 min the amount of Ca^{2+} ions incorporated into gyrolite crystal structure grows only to 248 mg of $Ca(OH)_2$/g.
2. The additive of gyrolite accelerates the early stage of hydration of OPC because of the adsorption reaction with both alkaline and Ca^{2+} ions. The decrease of Ca^{2+} ions in the solution accelerates the rate of dissolution of C_3S. This phenomenon was confirmed by a calculation of the apparent kinetic parameters of hydration at early age. It was determined that in the samples with gyrolite the induction period is effectively eliminated.
3. It was determined that gyrolite participate as chemical reagent in the OPC hydration. First, this compound binds alkaline ions and serves as a nucleation site for the formation of hydration products (stage I). Later on, the crystal lattice of gyrolite becomes unstable and turns into C–S–H, with higher basicity (C/S ~ 0.8). This recrystallization process is associated with the consumption of energy (the heat of reaction) and with a decrease in the rate of heat evolution of the second exothermic reaction (stage II). The experimental data and theoretical hypothesis were also confirmed by thermodynamic calculations.
4. The apparent kinetic parameters confirmed the proposed mechanism of OPC hydration with gyrolite additive. It was determined that when the amount of gyrolite is increased in the OPC samples, the reaction order $n_{app.}$ grows about 2.5 times (from 0.288 to 0.716), and the reaction rate $k_{app.}$ increases about 2 times (from 3.88 to 8.11).
5. The changes occur in the early stage of hydration of OPC samples and do not have a significant effect on the properties of cement stone. After 28 h of hardening, the mineralogical compositions of samples of pure OPC and OPC with additive are similar. It was found that the samples containing 2.5–7.5% gyrolite additive had a slightly higher compressive strength than OPC samples.

Acknowledgment

We gratefully thank Assoc. Prof. Dr. S. Kitrys — Head of Department of Physical Chemistry of KTU for constructive comments on kinetics and modeling of the hydration process section.

References

[1] H.M. Jennings, S.K. Johnson, Simulation of microstructure development during the hydration of a cement compound, J. Am. Ceram. Soc. 69 (1986) 790–795.
[2] J.J. Thomas, J.J. Biernacki, J.W. Bullard, S. Bishnoi, J.S. Dolado, G.W. Scherer, A. Luttge, Modeling and simulation of cement hydration kinetics and microstructure development, Cem. Concr. Res. 41 (2011) 1257–1278.
[3] A. Bezjak, Nuclei growth model in kinetic analysis of cement hydration, Cem. Concr. Res. 16 (1986) 605–609.
[4] E. Villa, P.R. Rios, Transformation kinetics for surface and bulk nucleation, Acta Mater. 58 (2010) 2752–2768.
[5] P.M. Dove, N. Han, J.J.D. Yoreo, Mechanisms of classical crystal growth theory explain quartz and silicate dissolution behavior, Proc. Natl. Acad. Sci. U. S. A. 102 (43) (2005) 15357–15362.
[6] J.W. Bullard, A determination of hydration mechanisms for tricalcium silicate using a kinetic cellular automaton model, J. Am. Ceram. Soc. 91 (2008) 2088–2097.
[7] S. Garrault, E. Finot, E. Lesniewska, A. Nonat, Study of C–S–H growth on C_3S surface during its early hydration, Mater. Struct. 38 (2005) 435–442.
[8] S. Bishnoi, K.L. Scrivener, Studying nucleation and growth kinetics of alite hydration using μ ic, Cem. Concr. Res. 39 (2009) 849–860.
[9] D.L. Kantro, S. Brunauer, C.H. Weise, Development of surface in the hydration of calcium silicates. II. Extension of investigations to earlier and later stages of hydration, J. Phys. Chem. 66 (1962) 1804–1809.
[10] E.M. Gartner, H.M. Jennings, Thermodynamics of calcium silicate hydrates and their solutions, J. Am. Ceram. Soc. 70 (1987) 743–749.
[11] R. Kondo, M. Daimon, Early hydration of tricalcium silicate: a solid reaction with induction and acceleration periods, J. Am. Ceram. Soc. 52 (1969) 503–508.
[12] P.W. Brown, E. Franz, G. Frohnsdorff, H.F.W. Taylor, Analyses of the aqueous phase during early C_3S hydration, Cem. Concr. Res. 14 (1984) 257–262.
[13] F. Bellman, D. Damidot, B. Möser, J. Skibsted, Improved evidence for the existence of intermediate phase during hydration of tricalcium silicate, Cem. Concr. Res. 40 (2010) 875–884.
[14] P. Fierens, J.P. Verhaegen, Hydration of tricalcium silicate in paste — kinetics of calcium ions dissolution in the aqueous phase, Cem. Concr. Res. 6 (1976) 337–342.
[15] I. Odler, H. Dörr, Early hydration of tricalcium silicate II. The induction period, Cem. Concr. Res. 9 (1979) 277–284.
[16] J. Zelic, D. Rusic, D. Veza, R. Krstulovic, The role of silica fume in the kinetics and mechanisms during the early stage of cement hydration, Cem. Concr. Res. 30 (2000) 1655–1662.
[17] J.A. Larbi, A.L.A. Fraay, J.M.J.M. Bijen, The chemistry of the pore fluid of silica fume-blended cement systems, Cem. Concr. Res. 20 (1990) 506–516.
[18] N.Y. Mostafa, P.W. Brown, Heat of hydration of high reactive pozzolans in blended cements: isothermal conduction calorimetry, Thermochim. Acta 435 (2005) 162–167.
[19] J.J. Thomas, H.M. Jennings, J.J. Chen, Influence of nucleation seeding on the hydration mechanisms of tricalcium silicate and cement, J. Phys. Chem. C 113 (2009) 4327–4334.
[20] J.W. Bullard, H.M. Jennings, R.A. Livingston, A. Nonat, G.W. Scherer, J.S. Schweitzer, K.L. Scrivener, J.J. Thomas, Mechanisms of cement hydration, Cem. Concr. Res. 41 (2011) 1208–1223.
[21] V. Morin, S. Garrault, F. Begarin, I. Dubois-Brugger, The influence of an ion-exchange resin on the kinetics of hydration of tricalcium silicate, Cem. Concr. Res. 40 (2010) 1459–1464.
[22] K. Ogawa, H. Uchikawa, K. Takemoto, I. Yasui, The mechanism of the hydration in the system C_3S–pozzolana, Cem. Concr. Res. 10 (1980) 683–696.
[23] J.W. Bullard, R.J. Flatt, New insights into the effect of calcium hydroxide precipitation on the kinetics of tricalcium silicate hydration, J. Am. Ceram. Soc. 93 (2010) 1894–1903.
[24] I.G. Richardson, The calcium silicate hydrates, Cem. Concr. Res. 38 (2008) 137–158.
[25] L. Black, K. Garbev, G. Beuchle, P. Stemmermann, D. Schild, X-ray photoelectron spectroscopic investigation of nanocrystalline calcium silicate hydrates synthesised by reactive milling, Cem. Concr. Res. 36 (2006) 1023–1031.
[26] J.J. Chen, J.J. Thomas, H.F.W. Taylor, H.M. Jennings, Solubility and structure of calcium silicate hydrate, Cem. Concr. Res. 34 (2004) 1499–1519.
[27] A. Hartmann, J.C. Buhl, K. van Breugel, Structure and phase investigations on crystallization of 11A tobermorite in lime sand pellets, Cem. Concr. Res. 37 (2007) 21–31.
[28] A. Nonat, The structure and stoichiometry of C–S–H, Cem. Concr. Res. 34 (2004) 1521–1528.
[29] J. Tits, K. Iijima, E. Wieland, G. Kamei, The uptake of radium by calcium silicate hydrates and hardened cement paste, Radiochim. Acta 94 (2006) 637–643.
[30] N.J. Coleman, Interactions of Cd(II) with waste-derived 11 A tobermorites, Sep. Purif. Technol. 48 (2006) 62–70.
[31] A. Stumm, K. Garbev, G. Beuchle, L. Black, P. Stemmermann, R. Nuesch, Incorporation of zinc into calcium silicate hydrates, part I: formation of C–S–H (I) with C/S = 2/3 and its isochemical counterpart gyrolite, Cem. Concr. Res. 35 (2005) 1665–1675.
[32] S. Shaw, C.M.B. Henderson, S.M. Clark, In-situ synchrotron study of the kinetics, thermodynamics, and reaction mechanisms of the hydrothermal crystallization of gyrolite, Am. Mineral. 87 (2002) 533–541.
[33] R. Jauberthie, M. Temimi, M. Laquerbe, Hydrothermal transformation of tobermorite gel to 10 angstrom tobermorite, Cem. Concr. Res. 26 (1996) 1335–1339.
[34] L. Stevula, M. Harman, I. Horvath, K. Putyera, The mineral gyrolite and its stability under hydrothermal conditions, Ceram. Silik. 4 (1990) 315–330.

[35] W. Nocun-Wczelik, Application of NMR in the studies of some autoclaved calcium silicate hydrates, synthesized with admixtures, in: W. Kurdowski (Ed.), Advances in Cement Chemistry Proc Inter Colloq, Kraków, 1997, pp. 59–66.
[36] R. Siauciunas, K. Baltakys, Formation of gyrolite during hydrothermal synthesis in the mixtures of CaO and amorphous SiO_2 or quartz, Cem. Concr. Res. 34 (2004) 2029–2036.
[37] M.A. Winters, J.D. Richter, S.L. Sagar, A.L. Lee, R.J. Lander, Plasmid DNA purification by selective calcium silicate adsorption of closely related impurities, Biotechnol. Progr. 19 (2003) 440–447.
[38] M.K. Doula, Simultaneous removal of Cu, Mn and Zn from drinking water with the use of clinoptilolite and its Fe-modified form, Water Res. 43 (2009) 3659–3672.
[39] B. Calvo, L. Canoira, F. Morante, J.M. Martinez-Bedia, C. Vinagre, J.E. Garcia-Gonzalez, J. Elsen, R. Alcantara, Continuous elimination of Pb^{2+}, Cu^{2+}, Zn^{2+}, H^+ and NH_4^+ from acidic waters by ionic exchange on natural zeolites, J. Hazard. Mater. 166 (2009) 619–627.
[40] E. Urbina-Sanchez, G.A. Baca-Castillo, R. Nunez-Escobar, M.T. Colinas-Leon, L. Tijerina-Chavez, J.L. Tirado-Torres, Tomato seedlings soilless culture on K^+, Ca^{2+} or Mg^{2+} loaded zeolite and different granule size, Agrociencia 40 (2006) 419–429.
[41] S.A. El-Korashy, Cation exchange of alkali metal hydroxides with some hydrothermally synthesized calcium silicate compounds, J. Ion Exch. 15 (2004) 2–9.
[42] V.S. Ramachandran, Differential thermal method of estimating calcium hydroxide in calcium silicate and cement pastes, Cem. Concr. Res. 9 (1979) 677–684.
[43] B.E.I. Abdelrazig, D.G. Bonner, D.V. Nowell, P.J. Egan, J.M. Dransfield, Estimation of the degree of hydration in modified ordinary Portland cement pastes by differential scanning calorimetry, Thermochim. Acta 145 (1989) 203–217.
[44] P. Juilland, E. Gallucci, R. Flatt, K. Scrivener, Dissolution theory applied to the induction period in alite hydration, Cem. Concr. Res. 40 (2010) 831–844.
[45] V.I. Babushkin, G.M. Matveev, O.P. Mchedlow-Petrossyan, Thermodynamics of Silicates, Stroyizdat Moscow, Russia, 1986.
[46] O. Levenspiel, Chemical Reaction Engineering, John Wiley & Sons, New York, 1999.